Role of Intermolecular Interactions on the Electronic and Geometric Structure of a Large π-Conjugated Molecule Adsorbed on a Metal Surface

L. Kilian,[1] A. Hauschild,[2] R. Temirov,[3,†] S. Soubatch,[3,†] A. Schöll,[1] A. Bendounan,[1] F. Reinert,[1] T.-L. Lee,[4] F. S. Tautz,[3,†] M. Sokolowski,[2,*] and E. Umbach[1]

[1]*Universität Würzburg, Experimentelle Physik II, Am Hubland, 97074 Würzburg, Germany*
[2]*Institut für Physikalische und Theoretische Chemie, Universität Bonn, Wegelerstr. 12, 53115 Bonn, Germany*
[3]*Jacobs University Bremen, School of Engineering and Science, PO Box 750761, 28725 Bremen, Germany*
[4]*European Synchrotron Radiation Facility, Bote Postale 220, 38043 Grenoble Cedex, France*

(Received 2 July 2007; published 2 April 2008)

The organic semiconductor molecule 3,4,9,10-perylene-tetracarboxylic-dianhydride (PTCDA) exhibits two adsorption states on the Ag(111) surface: one in a metastable disordered phase, prepared at low temperatures, the other in the long-range ordered monolayer phase obtained at room temperature. Notably, the two states differ substantial in their vertical bonding distances, intramolecular distortions, and electronic structures. The difference is explained by intermolecular interactions, which are particularly relevant for the long-range ordered phase, and which hence require attention.

DOI: 10.1103/PhysRevLett.100.136103 PACS numbers: 68.43.Fg, 68.37.Ef, 68.43.−h, 79.60.Dp

The bonding of large π-conjugated organic molecules to surfaces has attained widespread interest today. One motivation comes from the optimization of interfaces in organic thin film semiconductor devices, e.g., organic field effect transistors or light emitting diodes [1]. Another, more fundamental reason is that the adsorption of large π-conjugated organic molecules on surfaces bears novel aspects compared to the adsorption of small molecules [2]. These are related to the larger size of the molecules, the possible presence of different functional groups, and the specific properties of a system of delocalized π-electrons [3–6]. The new aspect, which we report here and which was neither expected nor quantified so far, is the significant influence that *intermolecular* interactions can have on the structural and electronic properties of a large π-conjugated molecule adsorbed on a surface.

The results were obtained for the prototype molecule 3,4,9,10-perylene-tetracarboxylic-dianhydride (PTCDA) adsorbed on the Ag(111) surface (see Fig. 1, inset). Up to today, mainly the long-range ordered, close packed monolayer of PTCDA on Ag(111) has been investigated, which is obtained for deposition on the sample at room temperature (RT). It will be referred to as the ''RT phase'' in the following. However, as we will report, PTCDA molecules can be prepared in a structurally and electronically different adsorption state, if the deposition is carried out at low sample temperatures.

Before we turn to these results, we briefly review main properties of the RT phase. Its unit cell is commensurate with the Ag(111) surface and contains two flat lying molecules on bridge sites, one of them being aligned with its long axis along the $[1\bar{1}0]$ direction (type A), the other one misaligned by 17° with respect to this direction (type B) [see Figs. 1 and 2(a)] [7,8]. The bonding to the Ag(111) surface occurs via chemisorption and involves the formation of PTCDA/Ag hybrid states. In particular, charge donation occurs from the Ag into the lowest unoccupied molecular orbital (LUMO), which is drawn partially below the Fermi edge, leading to a partially filled (''metallic'') hybrid state [8–10]. In addition, a geometric analysis yields a rather short bonding distance of the perylene core to the Ag and a distortion of the oxygen containing anhydride groups towards the Ag, in agreement with the noted scenario of a chemisorbed adsorbate [4].

The lateral arrangement of the molecules in the RT phase is of the *herringbone type*, and is driven by attractive intermolecular interactions between the negatively polarized oxygen containing anhydride groups and the positively polarized hydrogen terminated perylene cores of neighboring molecules. These intermolecular interactions involve several components which cannot be untangled: namely, (a) a direct covalent interaction due to orbital overlap, (b) an electrostatic interaction, (c) a van der Waals-type interaction, and (d) a substrate-mediated interaction which possibly involves the Ag(111) Shockley-type surface state.

Different to earlier experiments, the deposition was here done at low temperatures (LT), i.e., below 150 K. In order to avoid second layer effects, coverages up to ~70% of a monolayer of the RT phase were prepared. Further experimental information is given in Refs. [4,7–13]. Figure 1(a) displays a series of ultraviolet photoelectron spectroscopy (UPS) scans taken directly after preparation at 150 K, and for subsequent annealing steps up to 355 K. The three topmost PTCDA/Ag hybrid orbitals are marked ($L0$, $L1$, and $L2$). They mainly stem from the HOMO-1, the HOMO, and the LUMO orbital of the free PTCDA molecule. Upon annealing to RT, all three states continuously shift towards smaller binding energies. These shifts are a clear indication that PTCDA on Ag(111) at LT and after annealing to RT exhibits two different electronic states. Since the orbitals shift by different amounts, ranging from

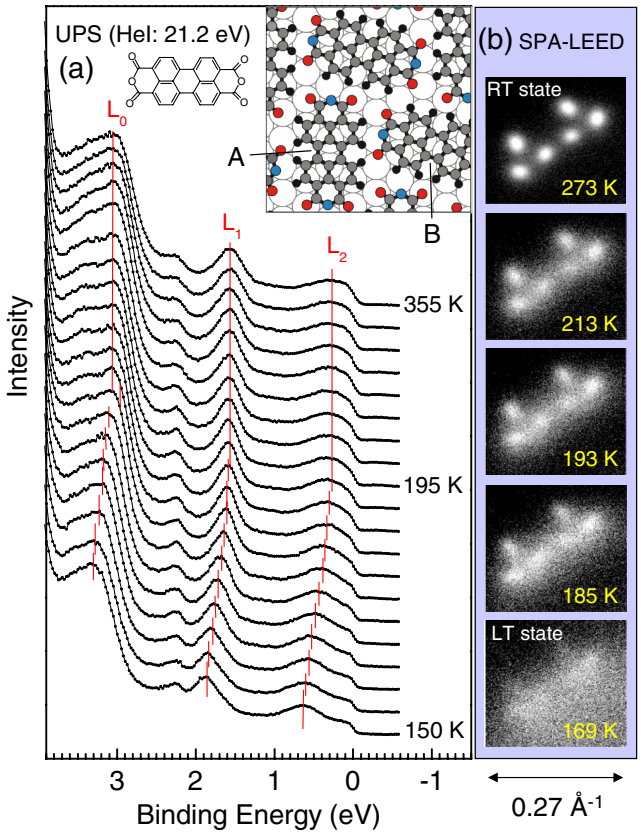

FIG. 1 (color online). (a) He-I UPS spectra (45° detection angle) for successive annealing steps up to 355 K after growth at 150 K. The vertical guide lines illustrate the shift of the three topmost PTCDA/Ag(111) hybride orbitals ($L0$, $L1$, and $L2$) upon the transition from the low temperature (LT) state to the room temperature (RT) state. The inset shows the structure of PTCDA and a hardsphere model of the herringbone structure in the RT phase. (b) High-resolution LEED scans of PTCDA superstructure spots (3rd and 4th order), taken for successive annealing steps, demonstrating the ordering. The original growth temperature was 147 K; the coverage 50%. The electron energy was 23.5 eV.

0.2 to 0.5 eV, a simple interpretation on the basis of a varying surface dipole electric field can be ruled out.

Directly after preparation at LT, low energy electron diffraction (LEED) images show *no* distinct superstructure spots. As illustrated in Fig. 1(b), LEED spots appear and sharpen at annealing temperatures between 170 and 200 K, until the diffraction pattern of the ordered RT phase is obtained [11]. This reveals that PTCDA deposited at low temperatures forms a disordered *metastable* state. Upon annealing, the layer gradually transits into the ordered RT phase via a series of intermediate states related to the increase of the next-nearest neighbor correlations (as seen from LEED). Upon a second cooling, the RT phase is maintained. In the following, the metastable, disordered PTCDA layer prepared at LT will be termed as "LT phase." Notably, the molecules in the LT phase deviate from isolated molecules, since they are subject to intermolecular interactions, although these are statistical (see below), and they deviate from molecules in the RT phase, since the latter are embedded in long-range ordered domains.

The inhibition of the RT phase at LT (100–150 K) is not simply a consequence of a too small rotational or lateral surface mobility of individual molecules, but is related to an energy barrier suppressing the local arrangement of the molecules into the herringbone structure. This can be seen from the scanning tunneling microscopy (STM) images in Figs. 2(b) and 2(c) taken on a low coverage LT phase. The PTCDA molecules are arranged in *dendritic clusters* of irregular shape and size. The azimuthal orientation of the molecules is peaked around two maxima along the $[1\bar{1}0]$ and $[2\bar{1}\,\bar{1}]$ directions of the substrate [Fig. 2(d), bottom panel]. Within the clusters, a preferential tail-to-edge arrangement between next-neighbor molecules is found [see Fig. 2(c)]. Between the clusters there are large areas of void

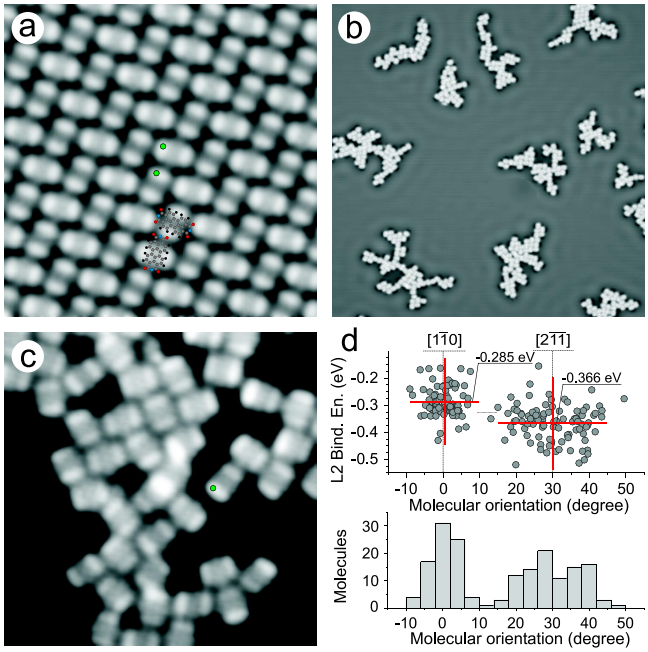

FIG. 2 (color online). STM images (recorded at 6–9 K) of (a) the room temperature (RT) and (b),(c) the low temperature (LT) phases of PTCDA on Ag(111). (a) Ordered herringbone island prepared by evaporation at 300 K and subsequent annealing at 550 K (RT phase). Image size 100 Å × 100 Å, $I = 16$ nA, $U_{\text{bias}} = -0.34$ V. (b) Dendritic islands of a layer of ~10% coverage deposited at 100 K. Image size 755 Å × 755 Å, $I =$ 100 pA, $U_{\text{bias}} = -0.34$ V. (c) Enlargement of part of a dendritic island prepared as in (b). Image size 100 Å × 100 Å, $I =$ 55 pA, $U_{\text{bias}} = -0.34$ V. (d) LT phase: reduced angular distribution of the PTCDA orientation (long axis of the molecule) with respect to the $[1\bar{1}0]$ direction of Ag(111) (bottom panel) and correlation of molecular orientation with $L2$ binding energy (top panel). 178 molecules within 3 dendritic islands have been evaluated. Red lines mark averages. Green dots in panels (a) and (c) mark the typical positions where the STS spectra have been recorded.

surface. These facts prove that rotational and lateral surface mobility is present for individual molecules after adsorption, even at these low temperatures.

What is the physical origin for the metastable LT phase of PTCDA on Ag(111)? At first glance, one may be tempted to consider it as a physisorbed "precursor" state, and explain the transition into the stable RT phase by the reorganization of the *interfacial* bonding geometry of individual molecules. *Intermolecular* interactions would be less important. However, this model does not apply for two reasons: (a) the LT state has to be considered as a second chemisorbed state, and (b) intermolecular interactions and the subsequent formation of the herringbone structure are responsible for the differences in the internal geometric and electronic structure of the two phases.

Evidence for a strong chemisorptive bonding of the LT state comes from its electronic structure and the vertical bonding geometry. The latter was determined for the RT and the LT state by the normal incidences x-ray standing wave (NIXSW) technique. The details of the analysis are described in refs. [4,14]. Figures 3(a) and 3(b) summarize the results. First of all, we find that the vertical bonding distance of the perylene core of the LT state (2.80 Å) is by 2.1% (0.06 Å) smaller compared to the RT state (2.86 Å), the difference being clearly beyond the error bar of the determination. This small bonding distance is strong evidence that the LT state is chemisorbed, too. For comparison, physisorbed PTCDA on Au(111) exhibits a much larger bonding distance of 3.27 Å [15]. However, we note that the NIXSW method integrates over the two types of molecules (*A* and *B*), which might have slightly different vertical heights. Additional support for a chemisorptive bonding is given by the internal vertical distortion of the LT state compared to the RT state: for the LT state the carboxylic O atoms are 0.31 Å below the perylene core, which is a significantly larger distortion than for the RT state (0.18 Å). For the RT state, this lowering of the carboxylic O atoms towards the surface was interpreted by the formation of bonds of the negatively polarized carboxylic O atoms to the Ag surface [4]. This indicates that there are significant local bonds to the Ag on the anhydride groups in the LT state, too.

To support our statement that the electronic and structural differences in the LT and RT phases are related to intermolecular interactions and lateral order, and not solely to differences in the interfacial bonding geometry, we systematically performed scanning tunneling spectroscopy (STS) on the hybrid orbital *L*2 for molecules in different local environments. In particular we have analyzed the correlation of the azimuthal molecular orientation, which is expected to monitor the variation in the interfacial bonding geometry, and the position of the maximum of the *L*2 orbital for isolated molecules, clustered molecules in the LT phase, and the two types of molecules the RT phase.

The *isolated* molecules (no neighbor within a radius of 10 Å) were produced artificially by "smearing out" an LT island with the STM tip. Both, isolated molecules and clustered molecules show the same orientational distribution with maxima along the $[1\bar{1}0]$- and $[2\bar{1}\,\bar{1}]$ direction [see Fig. 2(d) for the LT phase], independent of the scanning direction. Exemplary STS spectra for an isolated molecule and a molecule in the LT state are shown as the green and brown curves, respectively, in Fig. 3(c) [16]. As can be

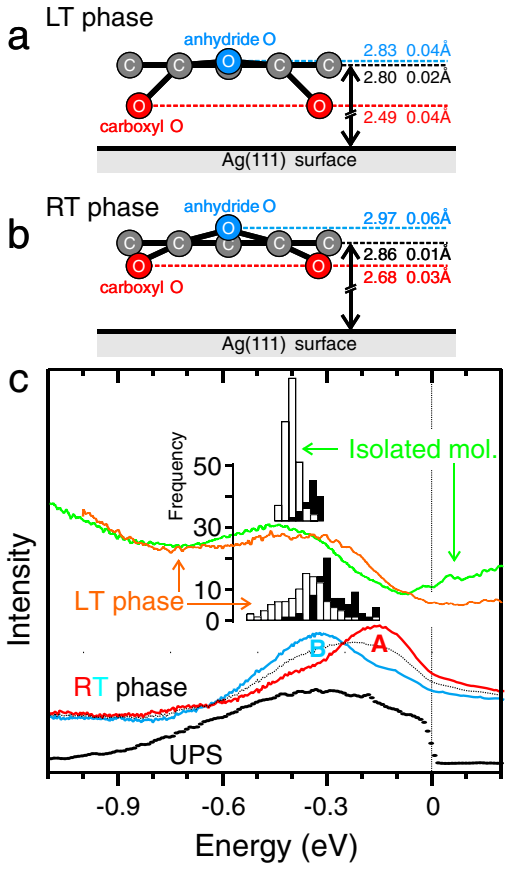

FIG. 3 (color online). Vertical configuration of PTCDA molecules in (a) the low temperature and (b) the room temperature phases as derived from NIXSW analysis. A side view onto the anhydride groups is presented. Gray: carbon atoms, blue: anhydride oxygen atoms, red: carboxylic oxygen atoms. The vertical length scale is expanded by a factor of 3. Data in (b) from Ref. [4]. (c) Spectroscopy of *L*2: High-resolution UPS spectrum, background corrected (black dots), measured at 40 K, 21.2 eV excitation energy, 40° detection angle, of 0.5 ML RT phase (prepared at 300 K), compared with STS spectra of type *A* (red, thick solid line) and type *B* (blue, dashed line) molecules in RT phase [Fig. 2(a)]. Thin dotted line: Superposition of the spectra for both types of molecules. Thick green/brown solid lines: STS spectra of an isolated and a molecule in the LT phase, respectively. Bar diagrams (width 20 meV): Energy distribution of peak *L*2 for isolated molecules (*top*, 142 molecules) and molecules in LT-phase (*bottom*, 178 molecules). Black bars: Molecules aligned within ±10° along $[1\bar{1}0]$. White bars: Molecules aligned within ±20° along $[2\bar{1}\,\bar{1}]$; cf. the statistical distribution in Fig. 2(d). STS spectra are taken under following conditions: $U_{\mathrm{mod}} = 4$ mV, $\nu_{\mathrm{mod}} = 1233$ Hz, $U_{\mathrm{bias}} = -340$ mV, $I = 0.16$ nA; at the positions of highest intensity of LUMO lobe, marked with the green dots in Figs. 2(a) and 2(c).

seen in Fig. 2(d) the $L2$ binding energies are clearly correlated to the azimuthal orientation for the LT phase. This demonstrates that the azimuthal orientation and hence interfacial effects influence $L2$ to some extent. This is also found for the isolated molecules. However, as illustrated by the bar diagrams in Fig. 3(c), the variation in the $L2$ peak position for isolated molecules is smaller and the center is at higher binding energies (-0.37 eV instead of -0.33 eV) compared to the LT phase. The broad distribution and actual positions of $L2$ of the disordered LT phase can evidently be only explained by a statistical variation of *lateral interactions*, since isolated and LT-phase molecules exhibit nearly the same orientational distribution on the surface.

Finally, we turn to the RT phase. STS spectra of the two types of molecules (A and B) in this phase are displayed in Fig. 3(c). Their maxima are 0.2 eV apart. The sum of the two spectra corresponds very well to the high-resolution UPS shown as the dotted gray curve in Fig. 3(c). In particular, we find that the $L2$ state of the aligned A type molecule is the one close to the Fermi edge and hence only partially filled and metal-like. The essential finding is now that this $L2$ state of molecule A lies essentially out of the distribution of energies of $L2$ observed for the LT phase [cf. Fig. 3(c)]. This suggests that this position of $L2$ is related to intermolecular interactions which are specifically related to the commensurate lateral order in the RT phase, since the statistical variation of local molecular interactions in the LT phase is too small to explain its position.

Clearly, a detailed interpretation of the interplay of the intermolecular interactions and the induced changes in the electronic and geometric structure is difficult. However, an argument based on the geometric structure is possible: As described earlier [4], negative partial charges on the anhydride groups cause the formation of bonds of the four carboxylic O atoms to the Ag, leading to the vertical distortion of the molecule. While these bonds are present in both phases, they seem to be strongly influenced by the herringbone-specific intermolecular interactions noted above [cf. Figs. 3(a) and 3(b)]. Possibly these withdraw some electron density from the carboxylic O atoms, weaken the O-Ag bonds and thus lower the intermolecular distortion, as it is experimentally observed. A further related consequence is an increase in the vertical bonding distance of the perylene cores with respect to the substrate. This goes hand in hand with a strong change of the $L2$ hybrid states of the A type molecule. A larger distance thereby leads to less charge transfer from the metal into the molecule and to a $L2$ position closer to the Fermi level. This effect may partly also account for the statistical variation of $L2$ in the LT state. Evidently, the effect on the electronic structure on the B type molecule is significantly smaller [see Fig. 3(c)]. This difference is however conceivable, since the distances of carboxylic O atoms to next-neighbor H atoms are different for the two types of molecules and substrate-mediated components may also differ due to the different adsorption sites [8].

In the above model, the activation barrier between the LT and the RT phase is related to the reorganization of the disordered network of intermolecular interactions in the LT phase and the concomitant relaxation of the internal distortion, loosening of the O-Ag bonds, and increase of the overall bonding distance to the substrate. However, the total energy gain is positive, since a larger energy than the activation energy is gained by forming the specific attractive intermolecular bonds, including their possible back-action on the interfacial bonds in the RT phase. We note that differential shifts for unoccupied orbitals of PTCDA were recently also reported for different ordered phases on stepped Au(111) surfaces [17]. However, since PTCDA is physisorbed on Au(111) [9,15], only a weak competition with the interfacial bonding is expected there. Nevertheless, we propose that the interplay between intermolecular interactions and the adsorption state described in our work is of general relevance for large π-conjugated organic molecules on surfaces and hence deserves attention, e.g., in theoretical calculations of these systems.

We thank C. Kumpf, C. Stadler, and J. Zegenhagen for helpful discussions and experimental assistance. Support by the ESRF and the DFG (SFB 624) is acknowledged.

*Corresponding author.
sokolowski@pc.uni-bonn.de
†Present address: Institut für Bio-und Nanosysteme 3, JARA, Forschungszentrum Jülich, 52425 Jülich, Germany.

[1] *Organic Electronics*, edited by H. Klauk (Wiley-VCH, Weinheim, 2006).
[2] S. M. Barlow and R. Raval, Surf. Sci. Rep. **50**, 201 (2003).
[3] A. Gerlach *et al.*, Phys. Rev. B **71**, 205425 (2005).
[4] A. Hauschild *et al.*, Phys. Rev. Lett. **94**, 036106 (2005); R. Rurali *et al.*, Phys. Rev. Lett. **95**, 209601 (2005); A. Hauschild *et al.*Phys. Rev. Lett. **95**, 209602 (2005).
[5] A. Alkauskas, A. Baratoff, and C. Bruder, Phys. Rev. B **73**, 165408 (2006).
[6] M. Preuss, W. G. Schmidt, and F. Bechstedt, Phys. Rev. Lett. **94**, 236102 (2005).
[7] K. Glöcker *et al.*, Surf. Sci. **405**, 1 (1998).
[8] A. Kraft *et al.*, Phys. Rev. B **74**, 041402(R) (2006).
[9] Y. Zou *et al.*, Surf. Sci. **600**, 1240 (2006).
[10] M. Eremtchenko, J. A. Schaefer, and F. S. Tautz, Nature (London) **425**, 602 (2003).
[11] L. Kilian, E. Umbach, and M. Sokolowski, Surf. Sci. **573**, 359 (2004).
[12] R. Temirov *et al.*, Nature (London) **444**, 350 (2006).
[13] A. Bendounan *et al.*, Phys. Rev. B **72**, 075407 (2005).
[14] A. Hauschild *et al.*, Phys. Rev. B (to be published).
[15] S. K. M. Henze *et al.*, Surf. Sci. **601**, 1566 (2007).
[16] We note that the position of $L2$ of the LT state in STS is found at an about $\sim$0.3 eV smaller binding energy compared to UPS. We suppose that this is due to a different coupling to vibronic excitations in the two techniques.
[17] J. Kröger *et al.*, Chem. Phys. Lett. **438**, 249 (2007).